Method for flood risk estimation in a tropical basin

Bettys Farias, Adriana Marquez, Edilberto Guevara and Demetrio Rey

ABSTRACT

This study proposes a method for estimating the flood risk in a tropical basin. The novelty consists of using two dynamic variables represented by the precipitation and the land use and land cover (LULC) to obtain the effective rainfall and its exceedance probability. The flood risk is determined by using deterministic methods depending on the exceedance probability of effective rainfall. Two time series of precipitation were involved. The first precipitation time series was used to prove the method corresponding to the months of the rainy season obtained from 58 gauging stations during the period 1980–2000. The second precipitation time series was applied for the validation stage of method corresponding to the period 2015–2018. In the validation stage, it has been found that there is a slight difference between the principal component N° 1 in the first time series with respect to the second time series. The method represents a contribution to determine the spatio-temporal distribution of flood risk that allows decisions to be taken to achieve preventive measures that contribute to the protection of human beings and goods.

Key words | effective rainfall, flood prediction, flood risk, prediction model

Bettys Farias
Adriana Marquez (corresponding author)
Edilberto Guevara
Center of Hydrological and Environmental Research,
University of Carabobo,
Naguanagua City,
Venezuela
E-mail: *ammarquez@uc.edu.ve*

Demetrio Rey
Institute of Mathematics and Compute Applied,
University of Carabobo,
Naguanagua City,
Venezuela

INTRODUCTION

Floods are one of the most frequent disaster risks, occurring yearly. Societies are subject to flood risks since flow paths associated to rivers move at a considerable distance in the main channel and overbank areas, especially in the floodplains (Guevara 2010). It is common to find human settlements of various social strata living under high flood risk. It is necessary to integrate actions that allow determination of the flood risks to alert the population living in vulnerable areas about the hazard to which they are exposed.

The traditional approach to dealing with the hydrological risks has been raised structural solutions; however, the use of structural measures has given scarce consideration to impacts of the social, cultural and environmental type that the hydraulic works cause. Although the historical merits of the structural measures have been the control of floods for the protection of urban settlements and the ability to use the floodplains for agricultural activities, their importance has diminished in recent decades. With respect to the non-structural measures, such as warning systems based on forecasting techniques in real time, the occupation restriction of floodplains for certain uses and flood-proof sites have received increasing attention (Farias *et al.* 2017). The application of spatial extrapolation techniques for specific data on variables of the natural environment is the basis for the development of geostatistics, which has been driven by the creation of integrated tools with geographic information systems (GIS) (Goovaerts 1997).

Since the beginning of the 21st century, most methods for estimating flood risk have been based on hazard and vulnerability analysis (Tables 1–3). The hazard is defined as the probability associated with the hydrological events that cause the occurrence of a flood, such as rainfall-runoff. Vulnerability is influenced by the socioeconomic characteristics of the population located in the flood zone. From 2004 to 2016, flood risk had been considered as a diffuse variable, inferred from vulnerability. The studies on the flood risk in that period presented maps of

doi: 10.2166/ws.2019.202

Table 1 | Results of the method of transformation of principal components expressed by eigenvalues from maps of flood risk during 1980–2000 in the Pao river basin, Venezuela

Period	Month	Principal components	PC1	PC2	PC3	PC4	PC5	PC6
Flood risk for $n = 5$ years								
1980–2000	May	Eigenvalues	0.34	0.15	0.098	0.076	0.059	0.045
		Accumulated proportion	36.00	51.81	62.00	69.86	76.03	80.68
1980–2000	June	Eigenvalues	0.25	0.19	0.085	0.077	0.052	0.045
		Accumulated proportion	31.20	55.37	66.07	75.72	82.25	87.97
1980–2000	July	Eigenvalues	0.24	0.14	0.081	0.060	0.054	0.037
		Accumulated proportion	31.72	49.66	60.05	67.82	74.76	79.61
1980–2000	August	Eigenvalues	0.24	0.18	0.12	0.096	0.067	0.054
		Accumulated proportion	28.70	50.25	65.22	76.40	84.17	90.47
1980–2000	September	Eigenvalues	0.26	0.19	0.08	0.07	0.05	0.04
		Accumulated proportion	29.07	50.51	60.10	68.02	74.38	79.34
1980–2000	October	Eigenvalues	0.32	0.18	0.12	0.06	0.05	0.04
		Accumulated proportion	36.06	56.93	70.02	76.49	81.81	86.51
Flood risk for $n = 50$ years								
1980–2000	May	Eigenvalues	0.17	0.09	0.06	0.04	0.027	0.023
		Accumulated proportion	29.84	45.81	56.81	65.02	69.72	73.71
1980–2000	June	Eigenvalues	0.17	0.075	0.055	0.031	0.027	0.023
		Accumulated proportion	37.98	54.23	66.03	72.80	78.71	83.77
1980–2000	July	Eigenvalues	0.16	0.092	0.038	0.029	0.027	0.024
		Accumulated proportion	35.20	55.32	63.73	70.05	76.02	81.14
1980–2000	August	Eigenvalues	0.13	0.086	0.064	0.029	0.022	0.017
		Accumulated proportion	30.22	50.02	64.78	71.54	76.66	80.76
1980–2000	September	Eigenvalues	0.168	0.107	0.077	0.034	0.027	0.024
		Accumulated proportion	31.14	50.92	65.20	71.64	76.71	81.22
1980–2000	October	Eigenvalues	0.237	0.128	0.073	0.041	0.033	0.022
		Accumulated proportion	37.84	58.25	69.99	76.56	81.90	85.42

hazard and vulnerabilities, both determined using empirical models. The hazard was estimated by two methods, (1) the zoning of susceptible areas to flooding (Garnica & Alcantara 2004) and (2) the combination of three variables (Kwak *et al.* 2011): (a) extreme discharge, (b) saturation deficit and (c) flood depth. The vulnerability has been estimated as socio-economic characteristics Garnica & Alcantara (2004), population possibly affected by floods (Kwak *et al.* 2011), or the combination of three variables (Balica *et al.* 2013): (1) exposure, (2) susceptibility and (3) resilience. Other studies proposed the warning of flood risk as a tool for hydrological forecasting, and a warning system in the basins (Hlavcova *et al.* 2005), as well as the spatial assessment of the flood risk in an area threatened by multiple sources of water including a copula-based approach for rainfall generation with spatial dependence and an integrated hydrological model for floods (Jiang *et al.* 2013). All these studies were characterized by the non-generation of a flood risk map.

Since 2016 to the present (Tables 1–3), flood risk maps have included as a qualitative variable derived from the empirical overlap of hazard and vulnerability (Vu & Ranzi 2017, Fiorillo & Tarchiani 2017). For 2016 and 2017, the hazard was represented by variables such as the intensity of the flood, and the probability associated with the occurrence of the rainfall- runoff process, likewise the flood risk index. Vulnerability has been associated mainly with the land use map (Vojtek & Vojteková 2016; Mojaddadi *et al.* 2017; Rawat *et al.* 2017). Allen *et al.* (2018), Zúñiga & Magaña (2018), Ghosh *et al.* (2019) proposed a variation of the traditional definition of flood risk, estimating it according to three variables, the two traditional ones (hazard and vulnerability) and the inclusion as a new variable of the exposure, which was considered through an

Table 2 | Comparison of flood risk methods

No.	Author	Maps	Model	Domain	Hazard	Vulnerability	Exposure	Risk	FR type
1	Garnica & Alcantara (2004)	1,2,3	1,3,4	2	1	1		1	
2	Hlavcova *et al.* (2005)	1	1	1					
3	Kwak *et al.* (2011)	1,3,4	1	2	2	2		1	
4	Balica *et al.* (2013)	3	1,2	2		3		1	
5	Jiang *et al.* (2013)	1	2	1					
6	Vojtek & Vojteková (2016)	2,3,5	1	2	3	4		1	1
7	Mojaddadi *et al.* (2017)	2,3,5	1	2	4	4		1	1
8	Rawat *et al.* (2017)	2,3,5	1	2	5	4		1	1
9	Vu & Ranzi (2017)	1	1						
10	Fiorillo & Tarchiani (2017)	1	1						
11	Allen *et al.* (2018)	5	1	2	5	1,5	1,2	2	1
12	Winter *et al.* (2018)	1	3	1	4	5		1	1
13	Zúñiga & Magaña (2018)	5	1	2	5	1,5		1	1
14	Ghosh *et al.* (2019)	5	1	2	5	1,5		1	1
15	Matheswaran *et al.* (2019)	5	3	2	5	1,5		1	1
16	Method proposed	5	2	2				3	2

index that depends on the density of the population and the housing. In addition, some computing tools have been created where the risk of flooding is estimated with a lumped approach (Hlavcova *et al.* 2005; Winter *et al.* 2018). Mainly, the flood risk has been computed using deterministic models and to a lesser extent through mixed and stochastic models (Garnica & Alcantara 2004; Matheswaran *et al.* 2019).

Table 3 | Codes for comparison of flood risk methods

	1	2	3	4	5
Maps	Non flood risk map	Hazard: zoning of áreas susceptible to flooding	Vulnerability	Population possibly affected by flooding	Flood risk
Model	Empirical	Deterministic: physical process	Stochastic	Mixed	
Domain	Lumped	Spatially distributed			
Hazard	Zoning of susceptible areas to flooding	(1) Extreme discharge, (2) Saturation deficit (3) Flood inundation depth	Flood intensity	Probability associated to rainfall-runoff	Flood hazard index
Vulnerability	Socio-economic characteristics	Population possibly affected by flooding	(1) Exposure (2) Susceptibility (3) Resilience	Land use map	Index
Exposure	Index	(1) Population density (2) Housing density			
Risk	(1) Hazard (2) Vulnerability	(1) Hazard (2) Vulnerability (3) Exposure	Exceedance probability of effective precipitation		
Flood risk type	Qualitative	Quantitative			

The current study has, as a novel purpose, the creation of a method to estimate the flood risk in a tropical basin. The method includes the estimation of the effective rainfall and the associations of this variable with the risk that the hydraulic structures designed to mitigate the flood events will be exceeded at least once during the useful life of the hydraulic works. Effective precipitation is an estimated variable using the Soil Conservation Service method of the United States (US-SCS). The advantage of using this method is that it includes dynamic variables such as precipitation and land use and coverage, which can be monitored by remote sensors within a telemetry or satellite network. The study unit where the method will be proved is the Pao river basin, Venezuela. The traditional techniques of change detection in land use and land cover have been applied in the Pao river basin in Venezuela, finding, by using post-classification, the following changes in the period 1986–2016 (Farias *et al.* 2018): (a) increases in urban use (1.37%) and agricultural (23%) and (b) decreases in classes of water bodies (0.55%), degraded soil (9.66%) and vegetation (8.1%). Likewise, the techniques for forecasting of changes in use and land cover have been developed based on the comparison of time series; it has been found that lower variance coefficients in the calibration process of statistical spatial prediction models are fit for obtaining land use and land cover (LULC) forecasting maps (Marquez *et al.* 2019).

METHODS

Figure 1 shows the method to estimate the flood risk in the study area from the monthly effective rainfall occurring in the basin of the Pao River. The methodology follows six stages: (1) estimation of the effective precipitation map; (2) generation of the effective precipitation classification map; (3) estimation of the exceedance probability map of the effective precipitation; (4) estimation of hydrological risk map; and (5) validation of method.

Estimation of map of effective rainfall

The estimation of the map of effective rainfall implies the obtaining of three preview maps: (1) precipitation, (2) map of water storage in the soil and (3) map of effective rainfall.

Estimation of map of precipitation

The precipitation data have been acquired in digital format from the website of the National Institute of Meteorology and Hydrology, Venezuela. The information is recorded every five minutes. Records of rain in each of the 25 selected gauging stations are accumulated on a monthly scale. An arrays of monthly precipitation time series have been created for the months from May until October within the rainy season from two periods, 1980–2000 and 2015–2018. In general, the dry period begins in November or December and ends in April or May in Venezuela (Ramirez 1971). The ArcGIS 10.0 computational tool has been used to transform tabular records to a layer of points, representing the geographical location of precipitation measurement stations inside and outside the Pao river basin. A geostatistical spatial tool is used to apply the ordinary Kriging method, and thus generate a map of monthly precipitation. The application of geostatistical techniques requires compliance with the following steps: (a) exploratory analysis, (b) structural analysis, and (c) predictions.

(a) ***The exploratory analysis*** allows verification of compliance with the principle of stationarity, extreme outliers, data normality by transformations, evaluation of variable distribution, and the identification of the existence of correlations among them. The adjustment of monthly precipitation to the normality distribution function is carried

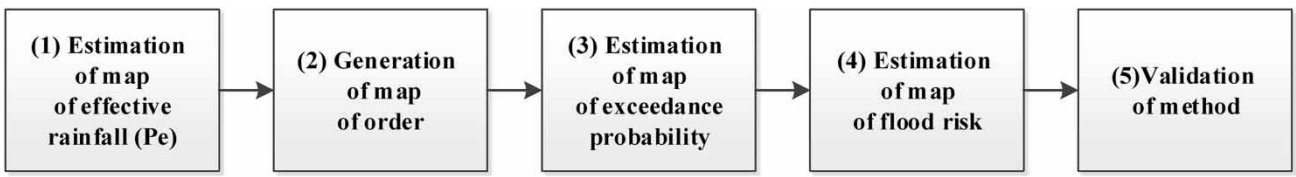

Figure 1 | Method for generation of map of flood risk.

out by obtaining properties derived from histograms such as the mean, median and asymmetry coefficient. In addition, the quantile-quantile graphic can be used to observe the quality of adjustment between the observations represented by dots and the linear relationship with a slope of 1:1.

(b) ***The structural analysis*** is applied using the tendency graphic of precipitation to determine its spatial variability, evaluating the presence of anisotropy, and determining variogram models for each variable, followed by its validation using the cross validation technique.

(c) ***Predictions:*** the models of semivariance statistical spatial prediction (SSPM) for predicting precipitation are applied; using the values of the target variable (z) at some new location s_0, being a set of observations of a target variable z denoted as $z(s_1)$, $z(s_2), \ldots, z(s_n)$, where $s_i = (x_i, y_i)$ is a location and x_i and y_i are the coordinates in geographical space and n is the number of observations. The precipitation values represent the target variable. The geographical domain of interest (area, land surface, object) can be denoted as A, represented by the Pao river basin. It defines inputs, outputs and the computational procedure to derive outputs based on the given inputs: $Z(s_0) = E\{Z/z(s_i), q_k(s_0), \gamma(h) s \epsilon A\}$

where $z(s_i)$ is the input point dataset, $q_k(s_0)$ is the list of deterministic predictors and $\gamma(h)$ is the covariance model defining the spatial autocorrelation structure. The type of SSPM used is the statistical model called Ordinary Kriging (OK), whose technique was developed by Krige (1951).

The predictions are based on the model:

$$Z(s) = \mu + \varepsilon'(s) \tag{1}$$

where μ is the constant stationary function (global mean) and $\varepsilon'(s)$ is the spatially correlated stochastic part of variation. The predictions are made as the analysis of point data is the derivation and plotting of the so-called semivariances – differences between the neighbouring values:

$$\gamma(h) = \frac{1}{2} E[(z(s_i) - z(s_{i+h}))^2] \tag{2}$$

where $z(s_i)$ is the value of target variable at some sampled location and $z(s_{i+h})$ is the value of the neighbor at distance (s_{i+h}).

The precipitation vector for a time (t_1) is an input for the geostatistical analyst tool into the GIS software; for this application, it is used ArcGIS v.10.0. The tool allows the selection of Ordinary Kriging as the method for the monthly precipitation spatial prediction. The predictor variables of precipitation are: precipitation semivariances and precipitation covariances. In this proposed method, the precipitation semivariances are an index of spatial auto-correlation. The semivariances can be explained by the following models: (a) Circular, (b) Spherical, (c) Tetraspherical, (d) Pentaspherical, (e) Exponential, (f) Gaussian, (g) Rational Quadratic, (h) K-Bessel, and (i) J-Bessel. The precipitation semivariance model is selected based on obtaining a gradient close to the unit, derived from the relation between the predicted precipitation and the observed precipitation. In addition, the graphics to assess the correlation include the four following statistics: Predicted versus Measured, Error versus Measured, Standardized Error versus Measured, and Standardized Error versus Normal. The best correlation between observed and predicted values is selected and the map of precipitation is obtained for a time (t_1).

Estimation of map of water storage in the soil

The equation used to estimate the water storage in the soil (S) is the corresponding method to the Soil Conservation Service of the United States (1986). The equation requires as input variables to the curve number (CN).

$$S = 25.4\left(\frac{1000}{CN} - 10\right) \tag{3}$$

The CN is obtained by superimposing the soil type and land use information; these two variables are represented on maps. The soil type map for the Pao river basin is obtained from the website of the Ministry of Environment and Natural Resources prepared for the Bolivarian Republic of Venezuela. This map is referenced geographically. A GIS tool of extraction by mask is applied using a polygon layer with the watershed limits. A new polygon layer is created to delineate the soil type within the watershed limits. The soil type layer is intersected with the land use and land

cover map. The term land use refers to how the land is being used by human beings. Land cover refers to the biophysical materials found on the land (Maidment & Djoikic 2000). The LULC map is generated through the application of the method of supervised classification using the maximum likelihood algorithm. This algorithm is applied using samples taken from profiles of spectral reflectance of an image whose bands have been stacked in an initial phase of the processing of satellite images, where the Pao river basin is contained (Farias *et al.* 2018). The satellite images are acquired from the website of the United States Geological Service from Landsat 8 OLI, which have received atmospheric, radiometric and topographic corrections. Once the soil type and LULC maps have been intersected, a new field is created in the attribute table of the layer named *CN*. This *CN* field is filled with the values given by the United States Soil Conservation Service (US-SCS). For filling of the *CN* field, a non-spatial table is created with the *CN* values for the LULC and soil type found in the study area. The non-spatial table is linked with the spatial table of attributes of the intersected layer of LULC and soil type using a common field. The reclassification tool is applied selecting the *CN* field, generating the *CN* map. The *CN* map is an input in Equation (3) by using the GIS Map Algebra tool to generate the *S* map.

Estimation of effective rainfall

The effective precipitation map is generated using the maps calculator tool contained in the Map Algebra menu in ArcGIS 10.0 software. The equation used to estimate the effective rainfall is the corresponding method of the Soil Conservation Service of the United States (1986). The equation requires as input variables to precipitation (*P*) and water storage in the soil (*S*).

$$P_e = \frac{(P - 0.2S)^2}{P + 0.8S} \tag{4}$$

where *P* and *S* maps are inputs in Equation (4).

Generation of map of order of the effective rainfall

The effective precipitation map is produced by applying the tool for reclassification contained in the tools of the spatial analysis module of the ArcGIS 10.0 program, which allows the values in a map to be changed. The input raster must have valid statistics. By default, the input raster is classified into nine classes for the reclassification table. If the input raster is a layer, the previous values of the reclassification will be obtained from the renderer. If the renderer extends, the reclassification will be set by default to 255 classes.

Estimation of map of the exceedance probability of effective rainfall

This is produced using the empirical method of design based on hydrological extreme events expressed by Equation (5) (Maidment & Djoikic 2000).

$$P(X \geq x_T) = m/n + 1 \tag{5}$$

where *m* is the order associated with the data from the series of effective precipitation and represented in the rating of the effective rain map obtained in step 2 and *n* is the number of data in the set of values of effective rain. An order map associated with the data from the series of effective precipitation is generated. The 'reclassify' tool is used to generate the order map. By this tool, an order is set to each effective precipitation value. The 1 value is associated to the maximum value in the P_e series. The effective precipitation series is ordered in a decreasing way. The exceedance probability map of effective precipitation is produced using the calculator tool for raster contained in the Map Algebra menu of the ArcGIS 10.0 software, where the order map of effective precipitation is the input for Equation (5).

Estimation of map of the flood risk

The flood risk is determined by using the equation of design for extreme hydrological events (Maidment & Djoikic 2000) indicated in Equation (6).

$$\bar{R} = 1 - [1 - (p(X \geq X_T)]^n \tag{6}$$

where, $(p(X \geq X_T)$ is the exceedance probability of the event of monthly effective precipitation, through its representation on the map. The random variable '*X*' is an

extreme event, when it is greater than or equal to a certain threshold value x_T. In this equation, the term x_T corresponds to the determined threshold value, n is the expected life of the structure; $\bar{R}$ is the probability that an event occurs at least once in n years. The return period 'T' of an event $X \geq x_T$, is the expected value of T, or the interval of 'average' recurrence between extreme events, equaling or exceeding a specified magnitude $X \geq x_T$. This hydrological risk map is produced using the calculator tool for raster contained in the map menu of ArcGIS 10.0 software, by including the exceedance probability as input.

Validation of method

In this study, the method validation is carried out by applying two statistical techniques of change detection, employing GIS tools in a sequence where the first technique used is based on principal components analysis (PCA) (Ingebritsen & Lyon 1985) followed by the second technique, which is related to the differencing of maps of the principal components (Singh 1989).

The PCA transforms a multivariate data set consisting of intercorrelated variables into a data set consisting of variables that are uncorrelated linear combinations of the original variables (Ingebritsen & Lyon 1985). The transformed variables are referred to as principal components (PCs). PCs are chosen in such a way that the first PC expresses the maximum possible proportion of the variance in the original data set; subsequent PCs account for successively smaller proportions of the remaining variance. The PCA is applied on two time series in two different periods of time related to the flood risk maps at a monthly scale to reduce the dimensionality in the spatio-temporal database. The two time series of monthly flood risk maps correspond to the rainy season during the periods of 1980–2000 and 2015–2018.

The second technique implies the PCs maps differencing that are spatially registered for the period of time t_1, and t_2, being subtracted, pixel by pixel, to produce a further map, which represents the change between the two periods of time corresponding to 1980–2000 and 2015–2018.

RESULTS AND DISCUSSION

Results of estimating the flood risk

Figure 2 shows the flood risk maps obtained using time series of rainy months during the period 1980–2000 for a hydraulic structure life of 5 years and 50 years (Equation (6)). The flood risk is categorized in five levels, considered as: very high (0.9–1), high (0.9–0.7), medium (0.7–0.5), low (0.5–0.3), and very low (0.3–0).

With respect to the flood risk maps obtained using time series of rainy months during the period 1980–2000 for a hydraulic structure life of 5 years, the results observed in the maps during the study period regarding the flood risk indicate that there is a trend to be found, from levels that vary between medium and very low in the urban zone (north-east region) and the water reservoirs (medium and low basin). In the rest of the basin, the flood risk is characterized as from high to very high where the LULC correspond to agriculture and vegetation, respectively. The results of estimating the flood risk for $n = 5$ years reproduce the pattern obtained in the maps of exceedance probability associated to the effective rainfall (Figure 1). In addition, the flood risk represents an approach to the exceedance probability when the exponent n trends to be the unit (Equation (6)). The effective rainfall is influenced by two variables linked to the precipitation and the CN parameter (Equation (3)), this last is obtained from LULC maps. It has been found that the CN parameter exerts an influence to delimit the spatial distribution of the effective rainfall; as a result the highest values occur in the paved zones, wet and water bodies of the basin.

With respect to the flood risk maps obtained using time series of rainy months during the period 1980–2000 for a hydraulic structure life of 50 years, the results observed in the maps during the study period regarding the flood risk indicate that the term associated to the mathematical expression of the non-exceedance probability significantly decreases as n is increased (Equation (6)). The final mathematical expression is approximated to the probability of exceedance, which represents the flood risk and is closed to the unit.

The highest probability of risk that the hydraulic work is exceeded at least once is obtained from the largest basin area covering areas of agricultural use and vegetation cover, which

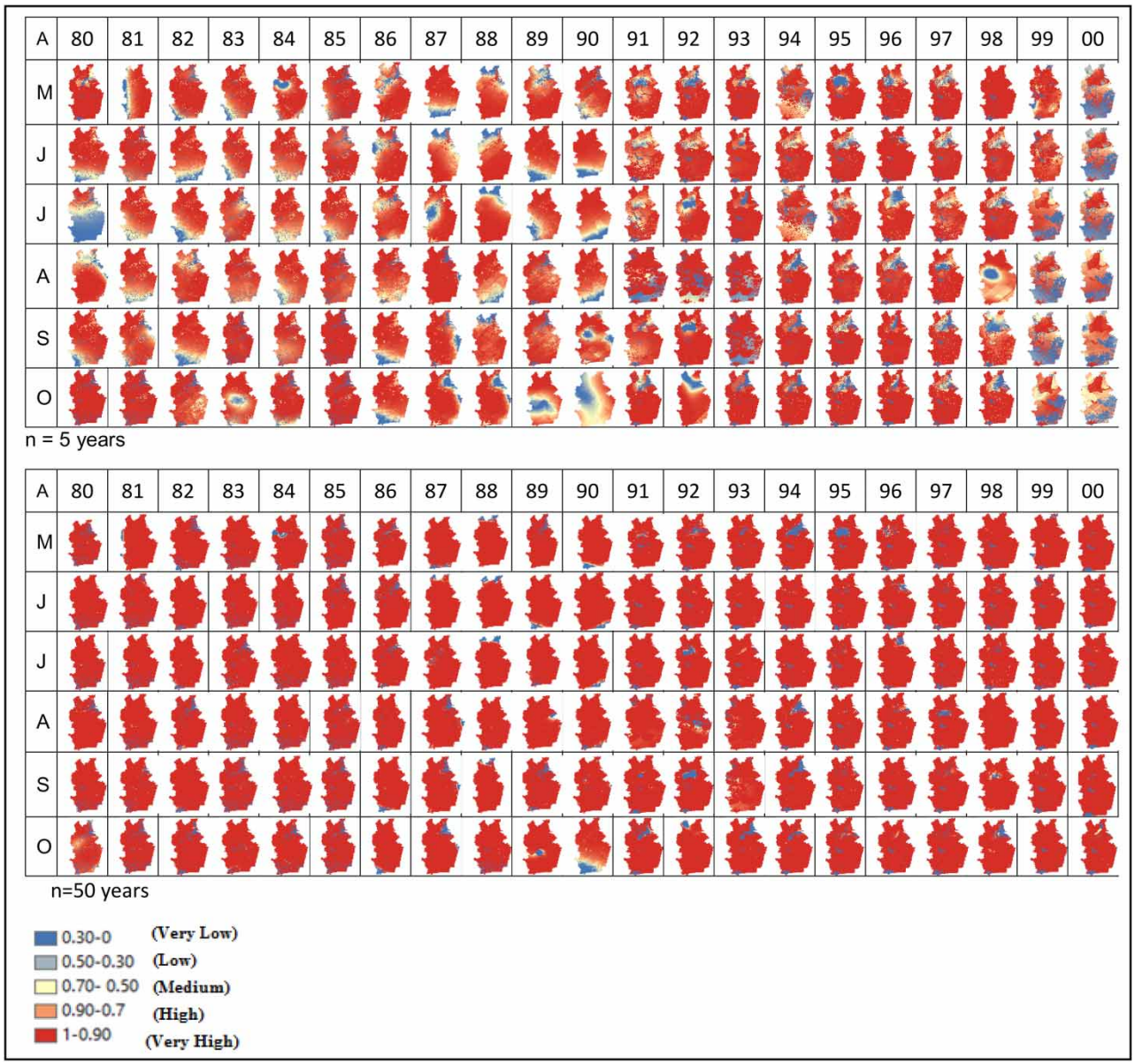

Figure 2 | Time series of flood risk for a useful life (n) of hydraulic works of $n = 5$ years and $n = 50$ years during the period 1980–2000 in the Pao river basin, Venezuela.

vary between 0.92 and 1. In these areas of high flood risk the lower effective precipitation occurs. The risk of exceedance for a projected hydraulic works decreases, ranging from 0 to 0.79 in urban areas where the effective rainfall occurs, with the highest values during the rainy season.

The flood risk model is sensitive to detecting as areas of moderate to low risk those of urban use and where there are hydraulic works for use and control of water. This is the case for the three water reservoirs built in the basin for water supply for human consumption, agriculture and as flood mitigation works. The sensitivity of the model is related to the fact that the CN is one of the highest in urbanized areas and bodies of water.

Results of analyzing the time series of flood risk

The results of analyzing the time series of flood risk are shown in Figure 3, represented by the principal components

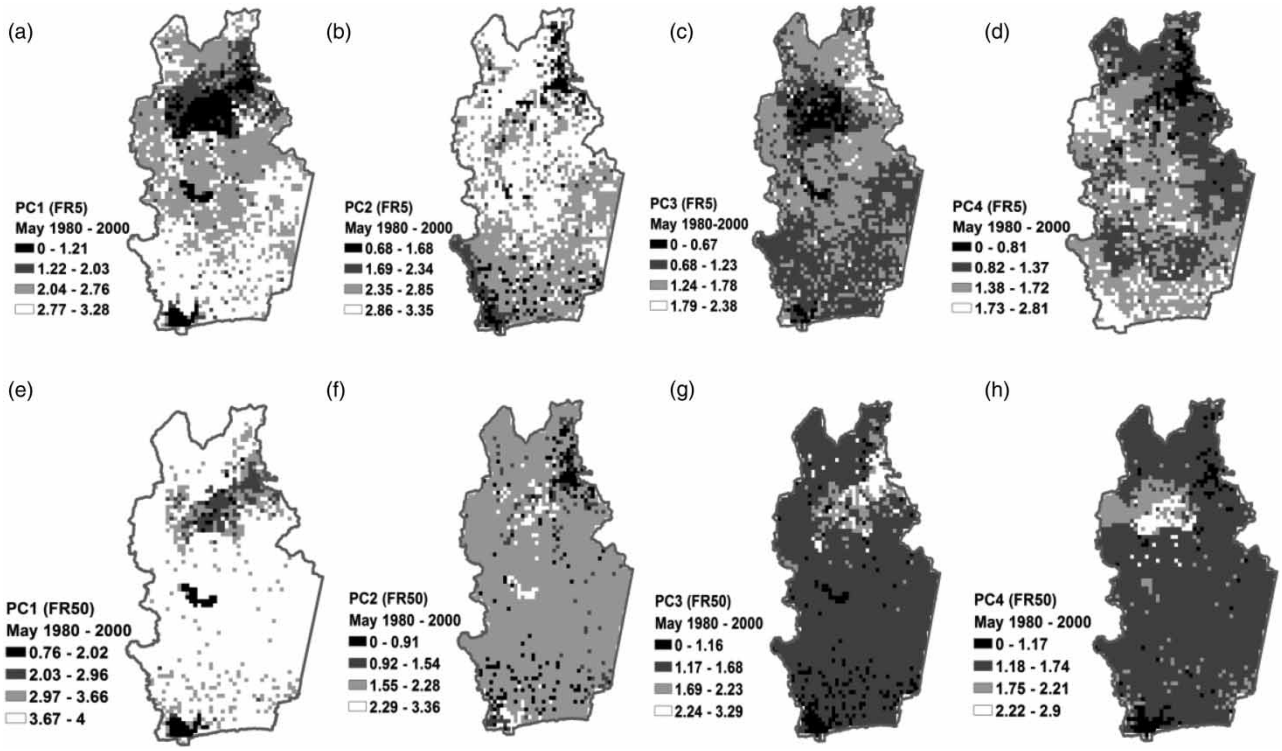

Figure 3 | Principal components (PCs) obtained from flood risk maps for May for the time series 1980–2000 in the Pao river basin, Venezuela: (a)–(d): PCs N°1 to N°4 for $n = 5$ years; (e)–(h) PCs N°1 to N°4 for $n = 50$ years.

(PCs) obtained from flood risk maps for the month of May for the time series 1980–2000 in the Pao river basin, Venezuela: (a–d): PCs N°1 to N°4 for $n = 5$ years. (e–h): PCs N°1 to N°4 for $n = 50$ years. Regarding PCs N°1 to N°4 for a useful hydraulic work life of $n = 5$ years (Tables 1 and 2), PC1 collects 36% of variation in the flood risk, PC2 contains 15.81% (accumulated 51.81%), PC3 10.19% (62%) and PC4 7.86% (69.86%). Figure 3(a) is confirmed by the principal components as the main variable, the observations found in the time series of flood risk (Figure 2). Figure 3(a) shows that the estimated flood risk, based on the time series of precipitation and classified satellite images in the period 1980–2000, was found to be located in the northeast and central region in a range from very low to low, occurring in the zones where the land uses are urban and land cover as water reservoirs take place. This PC1 map (Figure 3(a)) also shows that the flood risk categorized between medium and very high occurred in most of area proportion in basin along the study period. The PC2 shows in a better delineated form the spatial distribution of the flood risk in the urban zone evaluated at a very low level (black color). In general, the PC2 to PC4 show in a successively more diffuse way the location of the occurrence of flood risk in the Pao river basin.

The results of principal components for the flood risk estimated assigning the useful life of hydraulic works as 50 years through the period 1980–2000 show a pattern with respect to those found for $n = 5$ years (Figure 3(e)–3(h)). The zones of uses and coverages identified by urban and water reservoirs are mainly corresponding with the low flood risk. In this figure, the flood risk is classified in two extremes, being very low and very high. The PC1 (Figure 3(e)) contains the 29.84% of variance in the flood risk (Tables 1 and 2).

Tables 1 and 2 show the results of the method of transformation of principal components expressed by eigenvalues, which represent the variances of each PC derived from the maps of flood risk during the period 1980–2000

in the Pao river basin, Venezuela, for $n = 5$ years and $n = 50$ years. The vector of variances of PCs in the flood risk maps for a particular month within the rainy season is similar to each of those found among the six months within the rainy season (May–October), meaning that the variance is non-significant, and finding spatio-temporal pattern in the occurrence of the flood risk. The percentage of variance found in the flood risk represented by PC1 varies between 29 and 36% through the study period. As a sample, the vector of eigenvalues for May in the time series 1980–2000 for $n = 5$ years is PC1 (0.34), PC2 (0.15), PC3 (0.098), PC4 (0.076), PC5 (0.059) and PC6 (0.045).

Validation of results obtained in the time series of flood risk

The validation of results found in the PC N°1 derived from the flood risk map for the time series 1980–2000 using the updated flood risk map time series 2015–2018 by applying the change detection technique based on difference of PC N° 1 in the Pao river basin, Venezuela, is shown in Figure 4. In this figure it can be observed that the flood risk does not change the occurrence of the spatial pattern in a significant way. The of PC1's difference for the period taken as a sample, the month of October, between 1980–2000 (Figure 4(a)) and 2015–2018 (Figure 4(b)), gives as a result the map of Figure 4(c), which shows that PC1's difference is non-significant. This result can be explained because the pattern found in the period 1980–2000 corresponds to the current spatio-temporal distribution observed in the period 2015–2018, validating the method proposed and the areas committed in the extreme occurrence of flood risk.

The flood risk methods generated in other studies differ from the method proposed in the following aspects (Tables 1–3): (a) the flood risk does not appear as a direct variable represented in a spatially distributed way or grouped until 2016 (Garnica & Alcantara 2004; Hlavcova *et al.* 2005; Kwak *et al.* 2011; Balica *et al.* 2013); (b) combining of the traditional variables for the estimation of flood risk, such as hazard and vulnerability (Garnica & Alcantara 2004; Kwak *et al.* 2011); (c) qualitative empirical criteria for assessing the level of flood risk based on matrices with weighting criteria at scales; and (d) the lack of use of technological tools, such as remote sensing, that produce satellite images, digital elevation models, GIS computational tools used in LULC classification techniques, likewise geostatistical models.

The advantages of the proposed method for flood risk estimation consist of: (1) having inherent dynamics of changes in two variables of direct measurement in the field such as LULC and precipitation, (2) using advanced technology based on remote sensing, whose products are constituted of the satellite images from which a spatio-temporal distribution of LULC is obtained, (3) the application of a probabilistic method for the determination of exceedance probability of effective precipitation and (4) the implementation of the method in a GIS software by using a deterministic equation to obtain the spatio-temporal distribution of flood risk.

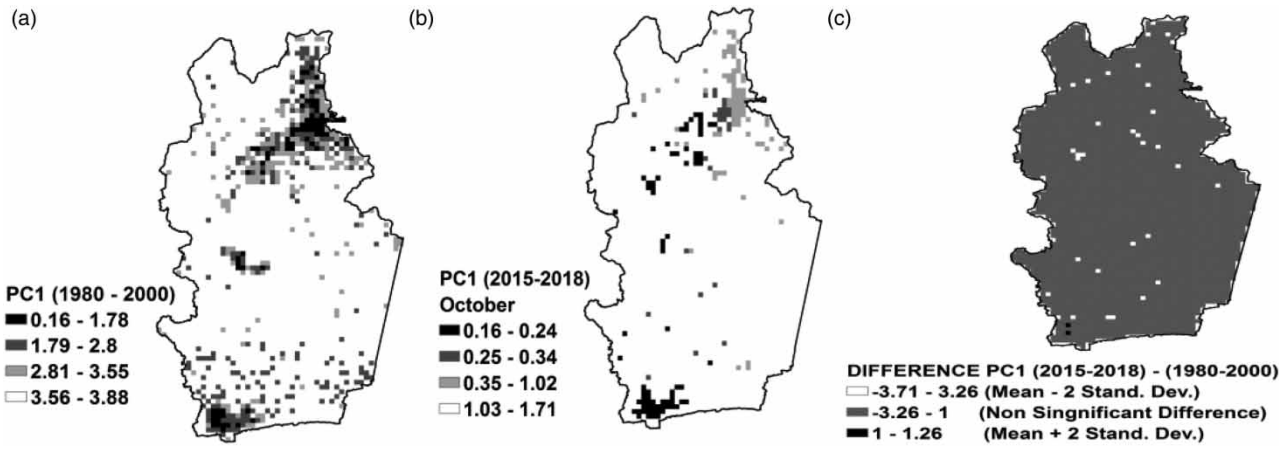

Figure 4 | Validation of results found in PC N°1 derived from the flood risk map for the time series 1980–2000 using the updated time series 2015–2018 of the flood risk map by applying the change detection technique based on difference of PC N° 1 in the Pao river basin, Venezuela.

CONCLUSIONS

The proposed method represents a contribution for the spatio-temporal estimation of the flood risk in river basins of tropical countries since it involves the exceedance probability of effective rainfall with the useful life of the hydraulic works. The estimating of flood risk is carried out by combining deterministic and stochastic models. The deterministic component is based on the curve number derived from land use and land cover maps, being a dynamic variable supported in satellite images. In addition, the geostatistical models are used for the spatio-temporal prediction of the precipitation. By combining the maps of spatio-temporal prediction of the curve number and precipitation, the effective rainfall is determined, representing the water depth in the flood zone.

The validation of the method is achieved by applying change detection techniques supported in the principal components (PCs) followed by applying the technique of the difference of PCs. The results of validation allow it to be demonstrated that there is a spatio-temporal pattern in the occurrence flood risk. The comparison of the results of flood risk time series compressed through the PCs between two time periods 1980–2000 and 2015–2018 could be indicating that there is not significant spatio-temmporal variance in the two main variables that influence the flood risk estimation, consisting of the precipitation and the land use and land cover.

The proposed method provides spatio-temporal information on the flood risk that allows decisions to be taken to apply preventive measures contributing to the protection of human beings and goods.

REFERENCES

Allen, S. K., Ballesteros-Canovas, J., Randhawa, S. S., Singha, A. K., Huggel, C. & Stoffel, M. 2018 Translating the concept of climate risk into an assessment framework to inform adaptation planning: insights from a pilot study of flood risk in Himachal Pradesh, Northern India. *Environmental Science & Policy* **87**, 1–10. https://doi.org/10.1016/j.envsci.2018.05.013.

Balica, S. F., Popescu, I., Beevers, L. & Wright, N. G. 2013 Parametric and physically based modelling techniques for flood risk and vulnerability assessment: a comparison. *Environmental Modelling & Software* **41**, 84–92. https://doi.org/10.1016/j.envsoft.2012.11.002.

Farias, B., Marquez, A., Guevara, E. & Romero, A. 2017 A methodology to prevent and deal with the hydrological risk in the northern area of the Naguanagua municipality state Carabobo - Venezuela. *Journal Encuentros. Unellez* **1** (1), 86–102.

Farias, B., Marquez, A., Guevara, E. & Rey, D. 2018 Characterization spatio–temporal land use in watershed using geomatic techniques. *Revista Ingenieria UC* **25** (1), 19–30. http://servicio.bc.uc.edu.ve/ingenieria/revista/v25n1/vol25n12018.pdf.

Fiorillo, E. & Tarchiani, V. 2017 *A Simplified Hydrological Method for Flood Risk Assessment at Sub-Basin Level in Niger. Renewing Local Planning to Face Climate Change in the Tropics*. Springer, Turin, Italy, p. 247.

Garnica Peña, R. J. & Alcantara Ayala, I. 2004 Flood risks associated with events of extraordinary precipitation in the course of the Río Tecolutla, Veracruz. *Geographical Research* **55**, 23–45. http://www.scielo.org.mx/scielo.php?pid= S0188-46112004000300003&script=sci_arttext&tlng=en.

Ghosh, A., Das, S., Ghosh, T. & Hazra, S. 2019 Risk of extreme events in delta environment: a case study of the Mahanadi delta. *Science of the Total Environment* **664**, 713–723. https://doi.org/10.1016/j.scitotenv.2019.01.390.

Goovaerts, P. 1997 *Geostatistics for Natural Resources Evaluation*. Oxford University Press on Demand, New York, NY, USA.

Guevara, E. 2010 *Management of Disasters*. Association of professors of the University of Carabobo, Valencia, Venezuela.

Hlavcova, H., Kohnova, S., Kubes, R., Szolgay, J. & Zvolensky, M. 2005 An empirical method for estimating future flood risks for flood warnings. *Hydrology and Earth System Sciences Discussions* **9** (4), 431–448. https://hal.archives-ouvertes.fr/hal-00304851.

Ingebritsen, S. E. & Lyon, R. J. P. 1985 Principal components analysis of multitemporal image pairs. *International Journal of Remote Sensing* **6** (5), 687–696. https://doi.org/10.1080/01431168508948491.

Jiang, X., Tatano, H. & Hori, T. 2013 A methodology for spatial flood risk assessment taking account of spatial-temporal characteristics of rainfall. *IDRiM Journal* **3** (1), 75–91. http://idrimjournal.com/index.php/idrim/article/view/57.

Krige, D. G. 1951 A statistical approach to some basic mine valuation problems on the Witwatersrand. *Journal of the Southern African Institute of Mining and Metallurgy* **52** (6), 119–139. https://hdl.handle.net/10520/AJA0038223X_4792.

Kwak, Y., Hasegawa, A., Inomata, H., Magome, J. & Takeuchi, K. F. K. 2011 A new assessment methodology for flood risk: A case study in the Indus River basin. In: *Risk in Water Resources Management: Proceedings of Symposium H03, IUGG2011*, Vol. 347, pp. 55–60. https://iahs.info/uploads/dms/16874.13-55-60-347-07-127_Youngjoo.pdf.

Maidment, D. R. & Djokic, D. 2000 *Hydrologic and Hydraulic Modeling Support: With Geographic Information Systems*. ESRI Inc., Redlands, CA, USA.

Márquez, A. M., Guevara, E. & Rey, D. 2019 Hybrid model for forecasting of changes in land use and land cover using satellite techniques. *IEEE Journal of Selected Topics in Applied Earth Observations and Remote Sensing* **12** (1), 252–273. https://ieeexplore.ieee.org/abstract/document/8605374/.

Matheswaran, K., Alahacoon, N., Pandey, R. & Amarnath, G. 2019 Flood risk assessment in South Asia to prioritize flood index insurance applications in Bihar, India. *Geomatics, Natural Hazards and Risk* **10** (1), 26–48. https://doi.org/10.1080/19475705.2018.1500495.

Mojaddadi, H., Pradhan, B., Nampak, H., Ahmad, N. & Ghazali, A. H. B. 2017 Ensemble machine-learning-based geospatial approach for flood risk assessment using multi-sensor remote-sensing data and GIS. Geomatics. *Natural Hazards and Risk* **8** (2), 1080–1102. https://doi.org/10.1080/19475705.2017.1294113.

Ramirez, L. E. 1971 *Development of a Procedure for Determining Spacial and Time Variations of Precipitation in Venezuela*. Reports. Paper 145. https://digitalcommons.usu.edu/water_rep/145/.

Rawat, P. K., Pant, C. C. & Bisht, S. 2017 Geospatial analysis of climate change and emerging flood disaster risk in fast urbanizing Himalayan foothill landscape. *Geomatics, Natural Hazards and Risk* **8** (2), 418–447. https://doi.org/10.1080/19475705.2016.1222314.

Singh, A. 1989 Review article digital change detection techniques using remotely-sensed data. *International Journal of Remote Sensing* **10** (6), 989–1003. https://doi.org/10.1080/01431168908903939.

Soil Conservation Service (1986) Urban hydrology for small watersheds. Technical Release **55**, 2–6. USDA (U.S. Department of Agriculture), Springfield, VA.

Vojtek, M. & Vojteková, J. 2016 Flood hazard and flood risk assessment at the local spatial scale: a case study. *Geomatics, Natural Hazards and Risk* **7** (6), 1973–1992. https://doi.org/10.1080/19475705.2016.1166874.

Vu, T. T. & Ranzi, R. 2017 Flood risk assessment and coping capacity of floods in central Vietnam. *Journal of Hydro-Environment Research* **14**, 44–60. https://doi.org/10.1016/j.jher.2016.06.001.

Winter, B., Schneeberger, K., Huttenlau, M. & Stötter, J. 2018 Sources of uncertainty in a probabilistic flood risk model. *Natural Hazards* **91** (2), 431–446. https://link.springer.com/article/10.1007/s11069-017-3135-5.

Zuniga, E. & Magaña, V. 2018 Vulnerability and risk for heavy rain in Mexico: the effect of the change in the coverage of the land use. *Geographical Research* **1** (95). http://dx.doi.org/10.14350/rig.59465.

First received 19 June 2019; accepted in revised form 15 December 2019. Available online 30 December 2019